International Journal for Housing Science and Its Applications
Publish August 10, 2025. Volume 46, Issue 4 Pages 6441-6454

https://doi.org/10.70517/ijhsa464547

Construction of concrete temperature estimation model in winter based on TimeGAN-SSA-TCN-BiLSTM-Attention

Rongsheng Han[1], Yue Jia[2,3], Changhe Shan[2,3,*], Yongjun Su[2,3] and Yu Wang[2,3]
[1] Hebei Water Conservancy Engineering Bureau Group Limited, Shijiazhuang, Hebei, 050021, China
[2] Department of Hydraulic Engineering, Hebei University of Water Resources and Electric Engineering, Cangzhou, Hebei, 061001, China
[3] Hebei Technology Innovation Center for Coastal Wetland Water Resources Allocation and Ecological Protection, Cangzhou, Hebei, 061001, China
Corresponding authors: (e-mail: 17333693541@163.com).

Abstract In North China, especially in Hebei Province, the low temperature and temperature difference in winter pose challenges to the construction of concrete structure of water conservancy projects. Timely monitoring of concrete internal temperature and effective control of temperature cracks are crucial to ensure the safety and stability of the structure. At present, the temperature monitoring of the concrete structure mainly relies on the embedded temperature sensor, but its high cost limits its wide application. Therefore, it is of great significance to construct the temperature estimation model of concrete structure to accurately grasp the temperature change law and prevent temperature cracks. In this paper, we study the winter construction project of Jianqiao Reservoir in Linxi County, Hebei Province, using the measured temperature data and regional temperature data to combine the temporal convolutional neural network (TCN) with the bidirectional long-short-term memory neural network (BiLSTM). Based on this, TimeGAN model and attention mechanism were introduced, and three optimization models, TSTBA, TLTBA and TMTBA, were constructed to further mine the data features. The results show that the introduction of TimeGAN model and attention mechanism significantly improves the model accuracy. Among the three optimized models, TSTBA, TLTBA and TMTBA models lead the performance in turn. Among them, the simulated values of the TSTBA model are highly consistent with the measured values in time and spatial distribution, and the simulated concrete temperature error range is between 0.099 and 0.191, with a high correlation coefficient. The accuracy of the deep neural network model reached 0.920, which effectively estimates the concrete temperature in winter. It provides solid theoretical support for the accurate evaluation of large concrete temperature change prediction and the effective management of concrete performance in water conservancy projects.

Index Terms concrete temperature, the combined deep learning models, the modified sparrow search algorithm, TimeGAN model, Attention mechanism

I. Introduction

In recent years, north China, especially Hebei Province, has been severely impacted by low temperatures, featuring wide diurnal temperature variations and intricate weather patterns, which have extremely adverse effects on the winter construction of concrete structures of water conservancy projects [1], [2]. In the concrete construction of large and medium-sized sluice base slab, temperature control and crack control are the key links of winter construction, which are directly related to the construction safety and stability of concrete structure [3], [4]. Therefore, timely and precise monitoring of the internal temperature of concrete structures, coupled with effective crack control measures, is crucial for ensuring the quality and mitigating temperature-induced cracks.

Currently, the primary means of monitoring concrete structure temperatures involves installing temperature sensors [5], [6]. While this approach ensures precise temperature monitoring, its significant cost hinders widespread adoption in large-scale projects [7]-[9]. In addition, the concrete pouring process is a complex heat exchange process, where the surface and the external environment constantly exchange heat, which is influenced by various factors, including external radiation, wind speed, humidity, temperature variations, and the inherent characteristics of the concrete structure [10], [11]. Therefore, the traditional empirical models have been unable to meet the requirements of high-precision temperature estimation.

To more accurately determine the temperature change trend of concrete structures, researchers proposed an estimation model, which was based on the relationship between temperature and environmental conditions, derived from field temperature measurements. This model was then applied to develop concrete temperature control measures. For example, Abid et al. (2016) [12] constructed a high-precision structural temperature estimation model based on the measured temperature data of the concrete structural beam for 14 months. Sheng et al. (2022) [13] Using finite element simulation, the vertical temperature estimation model of concrete in different areas was established, and the average absolute error and maximum absolute error are less than 1.0℃ and 1.5℃ respectively, indicating that the predicted temperature gradient is highly consistent with the simulated temperature gradient. In addition, Tan et al. (2024b) [14] developed an integrated learning model leveraging the strengths of random forest, support vector regression, and multilayer perceptrons to enhance predictive accuracy. The application of the perceptron and gradient-enhanced regression provides a valuable reference for conducting probabilistic analysis of temperature fields and investigating the long-term effects of temperature gradients, ultimately leading to a further reduction in prediction errors. In 2024, Wang et al. constructed a specific temperature estimation model based on the Pix2Pix model, and they verified its applicability and reliability through comparison with the strongly coupled heat-water-mechano-chemistry (THMC) model [15].

In order to further improve the accuracy of the temperature estimation model of concrete structures, this study takes the Yuemen project in the overwintering project in Zhongshan Irrigation District, Linxi County, Hebei Province. Leveraging the measured temperature data of the door panel and regional temperature data as input parameters, the study employs a temporal convolutional network (TCN) model and a bidirectional short-term memory (BiLSTM) model for predictive analysis. The model is improved by three new intelligent optimization algorithms, including an improved sparse search algorithm (SSA), Ivy League Optimization (IvL), and Moss Growth Optimization (MGO). Simultaneously, by integrating the TimeGAN model with an attention mechanism, we aim to further refine data feature extraction, ultimately establishing a highly accurate winter concrete temperature prediction model, to guide the engineering practice and improve the construction quality and management level of the concrete structure of water conservancy project.

II. Materials and methods

II. A.Project profile

Yuejin Gate is located in Jianzhong Irrigation District, Linxi County, Xingtai City, Hebei Province. It is an important part of the renovation, supporting facilities and water-saving renovation project of Jianzhong Irrigation District in Linxi County. Due to prolonged disrepair, the main structure of the sluice was unable to function as originally designed, prompting the decision to demolish and reconstruct the Yuejin Gate. The new sluice adopts a three-hole culvert structure with a designed flow rate of 30 m³ / s. The overall structure is designed according to the second-level standard, and the secondary structure is the third-level standard.

To ensure precise tracking of temperature variations within the concrete structure, thermocouples were strategically embedded at three distinct depths—upper, middle, and lower layers—prior to the construction phase. The elevations of each layer are 28.85 m, 28.20 m, and 27.55 m, respectively. Each layer has 49 thermocouples uniformly arranged, totaling 147, with their distribution and numbering detailed in Figure 1. Temperature monitoring work began on January 1,2024 and continued until February 29,2024. In the course of ongoing monitoring, the data collection system is programmed to automatically log temperature readings every two hours. Concurrently, it aggregates meteorological data specific to the construction site, encompassing ambient temperature, wind velocity, and humidity levels. This comprehensive approach ensures a thorough understanding of the concrete structure's thermal dynamics and its interplay with the surrounding environment.

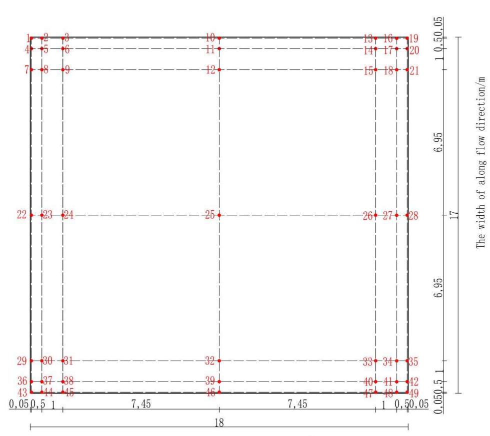

Note: In the figure, the red font is the number of temperature measurement points.

Figure 1: The location of the selected stations in Northeast China

II. B.Hybrid Deep Learning Model

The Temporal Convolutional Network (TCN) is a deep learning model used for processing time series data. The model effectively captures the long-distance dependence in the time series through techniques such as causal convolution and expansion convolution [16]. The TCN model mainly uses causal convolution, expansion convolution and residual connection to achieve the output results.

(1) Causal convolution

The information from before the current time point can be used in the model with causal convolution when predicting the output at the current time point, thereby avoiding information leakage. It can be defined as:

$$y_t = \sum_{t=0}^{K-1} h_t \cdot x_t \tag{1}$$

where K is the number of convolutional kernels; x_t is the input sequence; h_t is the convolutional kernel.

(2) Dilated convolution

Dilated convolution, also known as atrous convolution, expands the receptive field by introducing gaps or 'dilation rate' within the convolutional kernel. This allows the model to capture dependencies over a longer time range without increasing the number of parameters. It can be defined as:

$$y_t = \sum_{t=0}^{K-1} h_t \cdot x_{t-d} \tag{2}$$

where D is the dilation rate, with a value of 2; the meanings of the other parameters are the same as above.

(3) Residual connections

The TCN model can incorporate the residual block structure, utilizing skip connections to directly convey the input to the output. It can be defined as:

$$y_t = ReLU(x_t + Conv(Conv(x_t))) \tag{3}$$

where ReLU is the activation function; Conv represents the convolution operation.

The Bidirectional Long Short-Term Memory Network (BiLSTM) can be decomposed into two unidirectional Long Short-Term Memory Networks (Figure 2). In the processing of sequential data, richer contextual information is provided by the BiLSTM model through its ability to capture both forward and backward dependencies in the sequence simultaneously [17], [18].

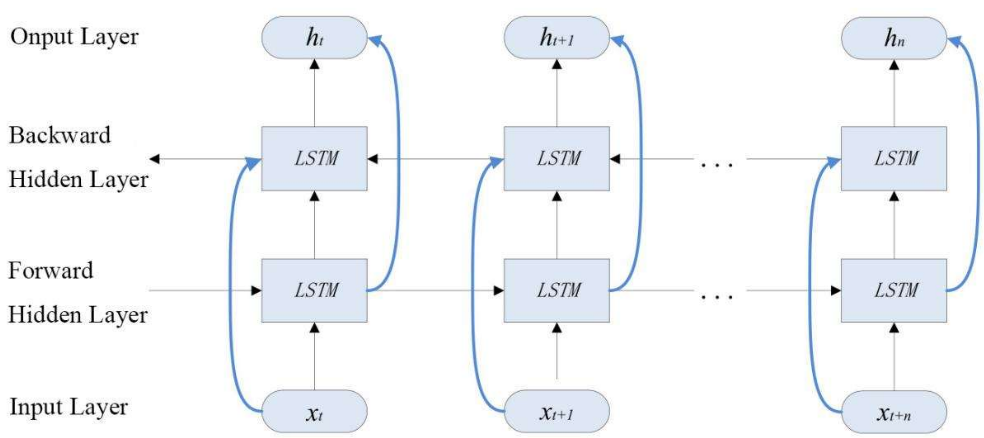

Figure 2: BiLSTM network structure

The TCN-BiLSTM (TB) model was constructed by combining the TCN model with the BiLSTM model. This model incorporates the temporal feature extraction capability of the TCN model and the bidirectional time series analysis capability of BiLSTM. The feature values were first extracted by the TCN model and then input into the BiLSTM model. The principle of the TB model is that:

(4) Convolutional Layer

Similar to the TCN model, the convolutional layer is responsible for extracting spatial features from the input data and generating feature maps. The ReLU activation function and the pooling layer work together to reduce the spatial dimension of the feature graph, thus helping to extract important features and reduce the computational burden.

(5) BiLSTM Layor

The feature parameters output by TCN are fed into a fully connected layer, subsequently integrated with the BiLSTM output, and processed by a BiLSTM-based architecture to yield the final prediction.

II. C.Sparrow Search Algorithm

The Sparrow Search Algorithm (SSA) is a swarm intelligence optimization algorithm which simulates the foraging behavior and predator-avoidance actions of sparrows. Proposed by Xue et al. in 2020, it draws inspiration from the natural foraging and anti-predation behaviors of sparrows [19]. The process of the algorithm can be defined as:

(1) Parameter initialization: The positions of a group of sparrows are randomly generated, and their fitness values are calculated.

(2) Explorer Update mechanism: According to the fitness value, some sparrows are selected as explorers, and they will update their position according to the current position and the global optimal position.

(3) Follower update: The followers update their positions based on the positions of the discoverers and their own fitness values.

(4) Reconnaissance forewarning: To simulate the alert behavior of sparrows, when a predator is detected, the sparrows will adopt an escape strategy and update their positions randomly to avoid being preyed upon.

In this paper, the SSA was optimized using a global optimization strategy. The process can be defined as:

(5) Chaotic sequence mapping initialization: The traditional SSA algorithm employed a random generation method for initialization. To enhance the algorithm's global search capability, chaotic sequences were utilized for population initialization.

(6) Butterfly optimization strategy was used to improve Explorer updates: The butterfly optimization strategy can update the positions in the algorithm based on the foraging behavior of butterflies. It can be defined as:

$$X_i^{t+1} = X_i^t + (r^2 X_{best} - X_i^t) f_i \tag{4}$$

where X_i^t and X_i^{t+1} are the positions of each particle; t is the number of iterations; X_{best} is the optimal position; f_i is the exploration trace; r is a random number falling [-1,1].

(7) The sine-cosine search strategy is adopted to optimize the position update of the followers: the sine and cosine functions can be optimized by using their oscillation characteristics, and then improve the convergence speed of the algorithm. The position update formula for the followers after improvement can be defined as:

$$X_i^{t+1} = \begin{cases} X_i^t + S_1 \times \sin(S_2) \times \left| S_3 \times X_{best} - X_i^t \right|, S_4 < 0.5 \\ X_i^t + S_1 \times \cos(S_2) \times \left| S_3 \times X_{best} - X_i^t \right|, S_4 \geq 0.5 \end{cases} \tag{5}$$

where S1, S2, S3, and S4 are all random numbers that follow a uniform distribution, respectively; the meanings of the other parameters are the same as above.

(8) Gaussian distribution was used to improve reconnaissance forewarning position updates: The Gaussian distribution performs well in local space search. Applying Gaussian perturbation to the global optimal individual helps the algorithm escape from local optima and also enhances its global search capability.

II. D.Ivy League Optimization Algorithm

The Ivy League Optimization Algorithm (IvL) is an optimization algorithm inspired by plant biology, specifically mimicking the growth, reproduction, and spread mechanisms of ivy plants [20]. Its operational process can be outlined as follows:

(1) Growth Phase: In this phase, the algorithm simulates the growth of ivy plants. The position update formula can be defined as:

$$X_{it}^{'} = X_{it} + \alpha \cdot \frac{X_{best} - X_{it}}{\| X_{best} - X_{it} \|} sin(\beta \cdot \| X_{best} - X_{it} \|) \tag{6}$$

where X_{it} and $X_{it}^{'}$ are the position of each particle; X_{best} is the global best position; α and β are parameters that control the step size and the oscillation, respectively.

(2) Propagation and Evolution Phase: In this phase, the algorithm introduces new individuals (seeds) into the population to enhance diversity. The formula can be defined as:

$$X_{new} = X_{best} + \gamma \cdot rand \cdot (X_{best} - X_{mean}) \tag{7}$$

where Xnew represents the new position in this phase, rand is a random number within the range [0,1], and Xmean denotes the mean position of the current population.

(3) Selection of Survivors: In this phase, the algorithm selects the best individuals based on their fitness values. The population size is maintained by replacing the worst individuals with the newly generated ones from the propagation phase.

II. E. Moss Growth Optimization

The Moss Growth Optimization (MGO) algorithm, drawing inspiration from the intricate growth mechanisms of moss found in nature [21], serves as a metaheuristic approach to seeking optimal solutions for complex problems. It mimics the growth and reproduction processes of moss to achieve this goal. The algorithm's process can be outlined as follows:

(1) Initialization: The algorithm starts with a random distribution of moss spores in the search space. Each spore represents a potential solution.

(2) Determination of Wind Direction: This mechanism determines the evolutionary direction of the population by partitioning the population and analyzing the positional relationship between individuals and the optimal individual. It helps avoid local optima traps.

(3) Spore Dispersal Search: This global exploration strategy simulates the dispersal of spores by wind. The position update formula can be defined as:

$$X_{new} = X_i + \sigma \cdot rand \cdot (X_{best} - X_i) \tag{8}$$

where X_i represents the position of each particle, rand denotes a random number within the range [0,1], σ serves as a scaling factor, and X_{best} indicates the global best position.

II. F. Development of a winter concrete temperature estimation model

The TimeGAN model classifies input data and subsequently extracts temporal features via its autoencoder and adversarial network mechanisms [22]. The Attention mechanism, by simulating the human attention span, focuses information extraction on key areas while automatically filtering out non-essential information [23]. The accuracy of estimation results in the concrete temperature model can be enhanced by incorporating the TimeGAN model. the Attention mechanism. The TB model, TimeGAN model, and Attention mechanism were respectively combined with the SSA algorithm, IvL algorithm, and MGO algorithm to construct the concrete temperature hybrid deep learning models TSTBA, TLTBA, and TMTBA. The TimeGAN model and the Attention mechanism were respectively combined with the TB model to construct the TimeGAN-TCN-BiLSTM-Attention model (TTBA) and the TCN-BiLSTM-Attention model (TBA). The construction process of the concrete temperature hybrid models was meticulously detailed.timation hybrid models can be defined as:

(1) Data Preprocessing: The input data were augmented using the TimeGAN model, and the augmented data were then fed into the TCN model structure.

(2) Parameter Optimization: The network weights and hyperparameters of models were optimized using the SSA, IvL, and MGO algorithms.

(3) TCN model output layer: The features of the input data were extracted based on the TCN model, and the extracted data were fed into the BiLSTM model.

(4) Output layer of BiLSTM model: In view of the bidirectional structure characteristics of BiLSTM model, we chose the tanh function as the non-linear activation function to realize the dimension transformation.

(5) Output output: The output result of the BiLSTM model is sent into the attention mechanism for weighted aggregation, so as to get the final model output.

II. G. Model training and testing

The air temperature and the concrete pouring time at different temperature measurement points were used as the input data for the models. The dataset was split into two periods: January 1st to 31st and February 1st to 29th, for model training and testing at each temperature measuring point. The models training and testing were performed using Matlab 2023a.

II. H. Statistical indicators

Relative root mean square error (RRMSE), coefficient of determination (R^2) and coefficient of efficiency (NS) were used to assess the temperature estimated models:

$$\mathrm{RRMSE} = \frac{\sqrt{\frac{1}{m}\sum_{i=1}^{m}(Y_i - X_i)^2}}{\bar{X}} \times 100\% \tag{9}$$

$$R^2 = \frac{\left[\sum_{i=1}^{m}(X_i - \bar{X})(Y_i - \bar{Y})\right]^2}{\sum_{i=1}^{m}(X_i - \bar{X})^2 \sum_{i=1}^{m}(Y_i - \bar{Y})^2} \tag{10}$$

$$NS = 1 - \frac{\sum_{i=1}^{m}(Y_i - X_i)^2}{\sum_{i=1}^{m}(X_i - \bar{X})^2} \tag{11}$$

where X_i and Y_i are the trained and estimated values, $\overline{X}$ and $\overline{Y}$ are the average value of X_i and Y_i.

The global performance indicator (GPI) was introduced to comprehensively evaluate the results of the model simulation [24], [25]:

$$GPI_i = \sum_{j=1}^{3} \alpha_j (g_j - y_{ij}) \tag{12}$$

where α_j is a coefficient, equaling 1 for RRMSE and -1 for Ens and R^2; g_j represents the median of j, while y_{ij} is the scaled value of j. The models with a higher GPI value indicated higher accuracy.

III. Results and discussion

III. A. Results

The fitting effect of various models to the concrete temperature is depicted in Figure 3. A detailed examination reveals that the temperature variation trend of the concrete structure, as simulated by each model, is fundamentally consistent, exhibiting a general pattern of initial increase followed by a decrease. However, there are significant differences in the fitting accuracy between the simulated and measured values of the different models. Among them, the TSTBA model had the highest accuracy of fitting the measurements in each region, followed by the TLTBA and TMTBA models. In particular, the maximum deviation between the simulated and measured values for the three concrete models was found to be 0.648°C, 3.499°C, and 4.755°C, respectively, which aligns with the temperature deviation standards and research findings in the field. Studies have shown that employing optimization algorithms, such as the response surface genetic algorithm and improved genetic algorithms, can significantly enhance the efficiency and accuracy of concrete temperature analysis, as evidenced by the improved fitting effect demonstrated in the data. In contrast, the maximum deviations of the TTBA, TBA, and TB models reached 5.173°C, 6.429°C, and 10.447°C, respectively. This shows that the introduction of the time growth model and attention mechanism has had a positive impact on enhancing the fitting accuracy of concrete temperature predictions. In summary, the TSTBA model showed the best fit in all models.

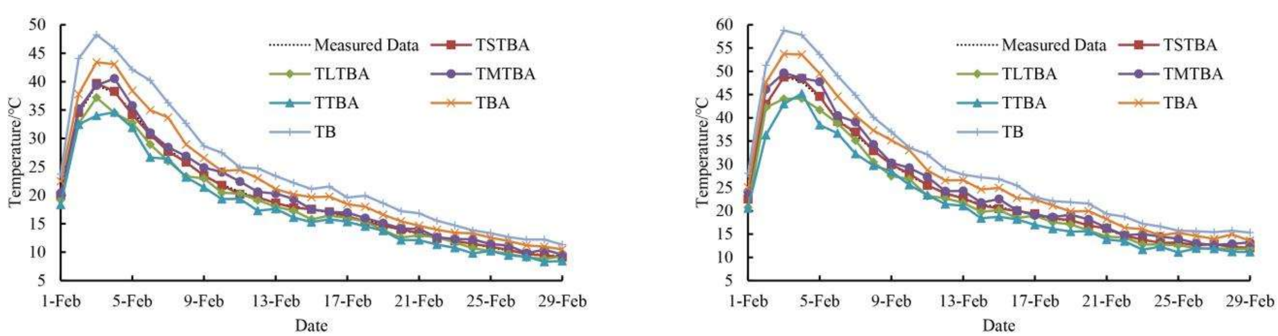

(a) The upper layor

(b) The middle layor

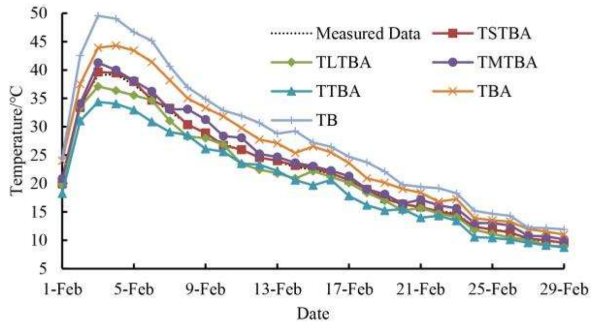

(c) The lower layor

Figure 3: Comparison of fitting effects of concrete temperature in winter simulated by different models, with a focus on the accuracy of the simulation results compared to actual measurements

Figure 4 shows the violin diagram of the simulation accuracy of different models on the upper concrete temperature, and Table 1 lists the corresponding accuracy indicators in detail. The data show that the three algorithms can effectively improve the simulation accuracy of the model. Among them, the TSTBA model simulates the upper temperature of concrete slab, with its RRMSE, ENS, NS and GPI indexes of 0.144,0.960,0.946 and 1.316, respectively, with the lowest error and the highest consistency among all models. The TLTBA model was second, with its RRMSE, ENS, NS, and GPI values of 0.175,0.936,0.926, and 0.961, respectively. Nonetheless, among models optimized by the three algorithms, the TMTBA model exhibited a notably lower accuracy, specifically a GPI of 0.317. This shows that the combination of the TimeGAN model with the attention mechanism can significantly improve the simulation accuracy of the model. Conversely, the GPI values for the TTBA, TBA, and TB models were -0.316, -0.805, and -1.685, respectively, thereby further confirming the effectiveness of our optimization algorithm.

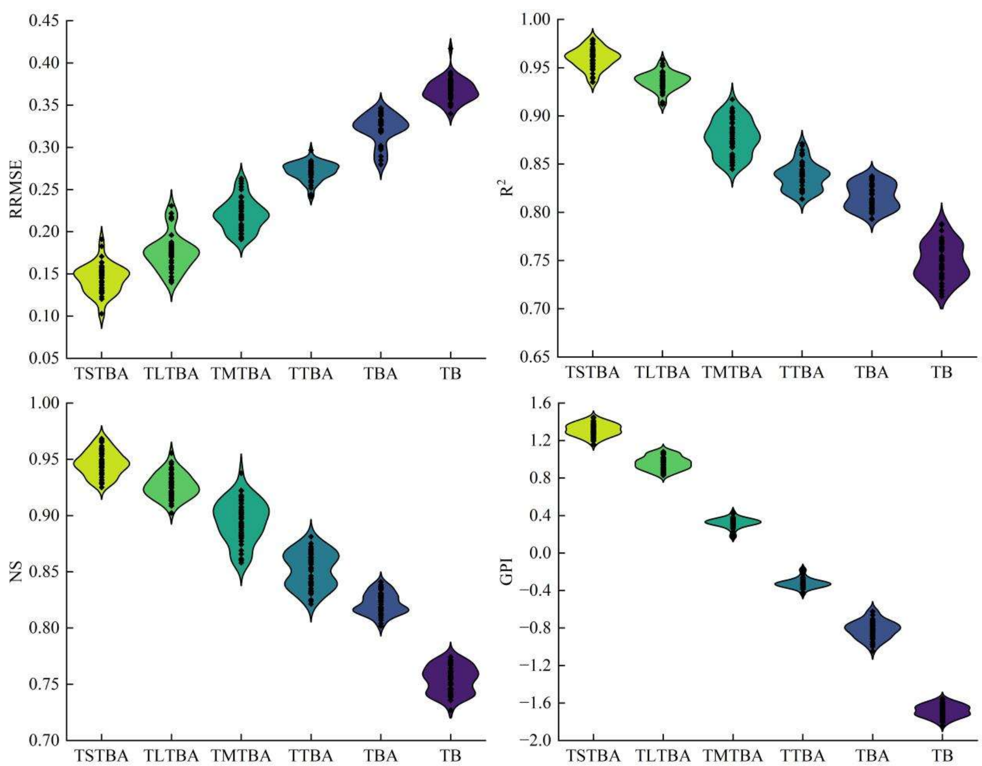

Figure 4: The accuracy of the simulated temperature of the upper layer of the concrete slab using different models

Table 1: Comparison of the accuracy in simulating concrete temperature profiles using different models

Partition	Models	RRMSE	R2	NS	GPI
The upper layor	TSTBA	0.144	0.960	0.946	1.316
	TLTBA	0.175	0.936	0.926	0.961
	TMTBA	0.219	0.878	0.895	0.317
	TTBA	0.271	0.837	0.852	-0.316
	TBA	0.321	0.817	0.821	-0.805
	TB	0.367	0.749	0.754	-1.685
The middle layor	TSTBA	0.144	0.962	0.956	1.475
	TLTBA	0.173	0.931	0.926	1.035
	TMTBA	0.221	0.882	0.877	0.314
	TTBA	0.270	0.845	0.834	-0.314
	TBA	0.316	0.808	0.814	-0.831
	TB	0.351	0.757	0.757	-1.525
The lower layor	TSTBA	0.140	0.950	0.942	1.298
	TLTBA	0.171	0.914	0.917	0.849
	TMTBA	0.212	0.875	0.881	0.275
	TTBA	0.263	0.842	0.851	-0.275
	TBA	0.302	0.795	0.798	-0.951
	TB	0.354	0.756	0.736	-1.702

Figure 5 illustrates the violin plot of simulation accuracy for various models predicting the temperature at the middle layer of concrete, with Table 1 detailing the corresponding accuracy metrics. For instance, research such as that presented in Reference 0 has shown that the composite exponential model generally outperforms other models in accurately describing the adiabatic temperature rise of concrete, which is crucial for effective temperature field and stress field simulation. Studies have shown that the TSTBA model excels in accurately simulating the temperature of the middle layer of concrete slabs, with its performance metrics such as RRMSE (0.144), ENS (0.962), NS (0.956), and GPI (1.475) ranking it at the forefront among various models. The TLTBA model followed closely with its accuracy indicators. Nevertheless, the accuracy of the TMTBA model was relatively low in the models optimized by the three algorithms. In addition, it is found that the introduction of TimeGAN model and attention mechanism has effectively improved the simulation accuracy of the model. Specifically, the TTBA model decreased by RRMSE 16.86%, and the ENS and NS increased by 0.16% and 0.15%, respectively. Compared with the TB model, the RRMSE of the TBA model has decreased by 9.47%, but the ENS and NS have decreased by 6.74% and 7.59%, respectively.

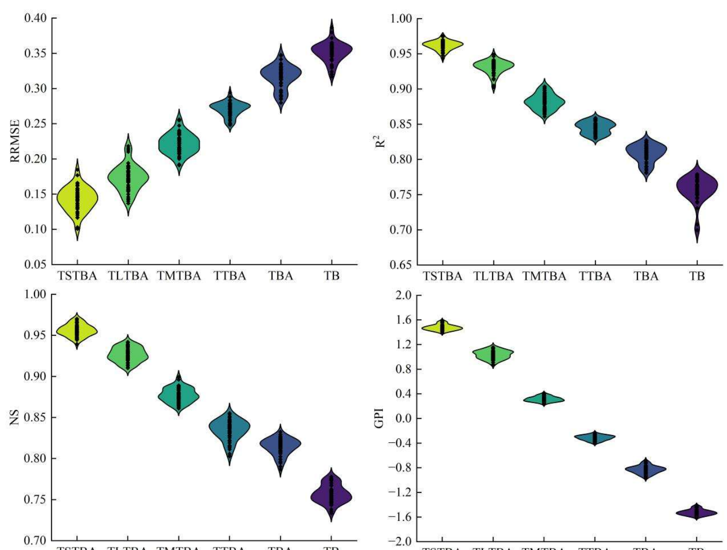

Figure 5: The accuracy of the simulated temperature of the middle layer of the concrete slab using different models, as validated by numerical analysis and comparison with experimental data

Figure 6 shows the violin diagram of the simulation accuracy of different models on the lower concrete temperature, and Table 1 also gives the corresponding accuracy index. Data shows the TSTBA model topped in simulation accuracy for lower concrete plate temperature, achieving RRMSE of 0.140, ENS of 0.950, NS of 0.942, and GPI of 1.298. The TLTBA model is the second, and its accuracy index is also quite excellent. The combination of the TimeGAN model and the attention mechanism significantly enhances the simulation accuracy of the model, whereas the TB model demonstrates comparatively lower accuracy across all models.

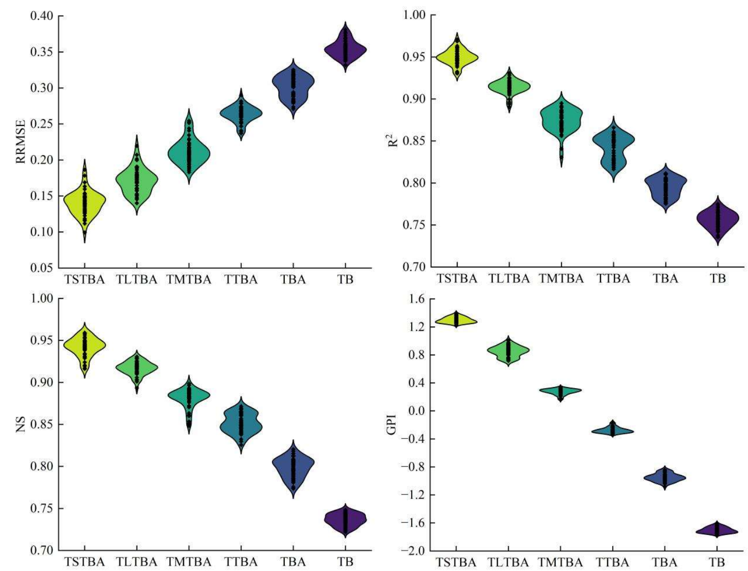

Figure 6: The accuracy of the simulated temperature of the lower layer of the concrete slab using different models

Figure 7 shows the spatial distribution of the temperature accuracy in the upper layers of different models. As can be observed from the chart, the RRMSE values for different models are generally higher in the central area and relatively lower in the edge areas. Specifically, the RRMSE values of the TSTBA model were generally lower in the upper layer of the plate, ranging from 0.103 to 0.191, with the highest value appearing around the temperature measurement point 25 and the lowest value around point 43. The RRMSE values of the TLTBA model were higher than the TSTBA model, ranging from 0.140 to 0.231. The RRMSE values of the TMTBA model in the upper plate range from 0.191 to 0.263, which are considered to be within an acceptable range for most applications, as RMSE values are typically expected to be between 0 and 1. Furthermore, the incorporation of the TimeGAN model and attention mechanism significantly enhanced model accuracy, resulting in the TTBA model boasting a lower RRMSE value compared to both the TBA and TB models. Concurrently, the ENS and NS values of various models exhibited a pattern of decreased central values and increased edge values. The TSTBA model exhibited excellent performance in both indicators.

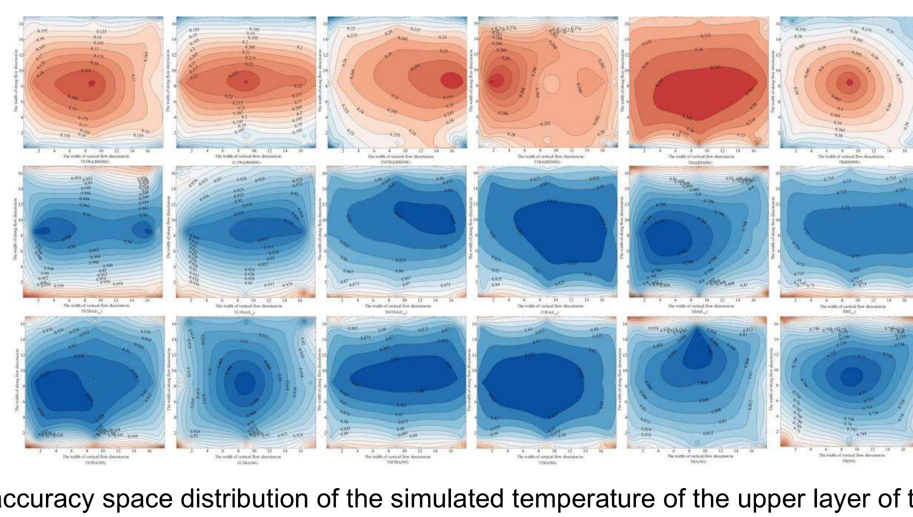

Figure 7: The accuracy space distribution of the simulated temperature of the upper layer of the concrete slab using different models, as compared with actual measurements and experimental studies

Figure 8 shows the spatial distribution of temperature accuracy in the middle layer of different models. The figure reveals that RRMSE values for various models in the middle layer exhibit a central peak, decreasing towards the edges. Notably, the TSTBA model demonstrates lower RRMSE values, spanning 0.101 to 0.185. In contrast, the TLTBA model exhibits higher RRMSE values, ranging between 0.137 and 0.218, compared to the TSTBA model. The RRMSE of the TMTBA model in the middle layer of the plate ranged from 0.199 to 0.256. Similarly, the incorporation of the TimeGAN model and the attention mechanism significantly enhances the model's accuracy. In addition, the ENS and NS in the middle level of different models also showed similar spatial distribution rules to RRMSE, and the TSTBA model is dominant in these two indexes.

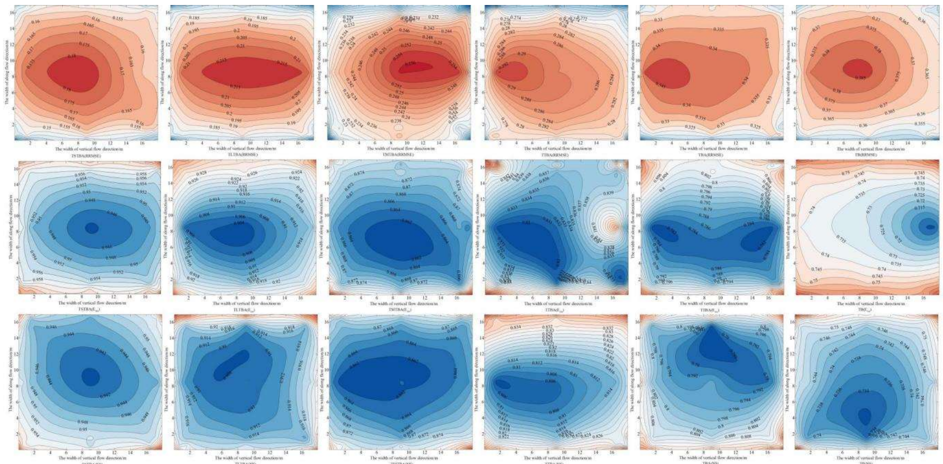

Figure 8: The accuracy space distribution of the simulated temperature of the middle layer of the concrete slab using different models

Figure 9 presents the spatial distribution of the accuracy of simulating the temperature beneath the slab for different models. The figure reveals a trend in RRMSE values, with higher values concentrated in the central part and lower values at the edges for the various models. Among them, the TSTBA model has relatively low RRMSE values in the lower layer of the slab, ranging from 0.099 to 0.186. In contrast, the TLTBA model exhibits higher RRMSE values, spanning from 0.140 to 0.220, compared to the TSTBA model. The RRMSE range for the TMTBA model in the lower layer of the slab is 0.183 to 0.254. At the same time, the ENS and NS values of different models also exhibit spatial distribution characteristics similar to those of the relative root mean square error (RRMSE). Specifically, the ENS and NS values of the TSTBA model remain at high levels in the lower layer of the slab, further confirming its superiority in simulating concrete temperatures.

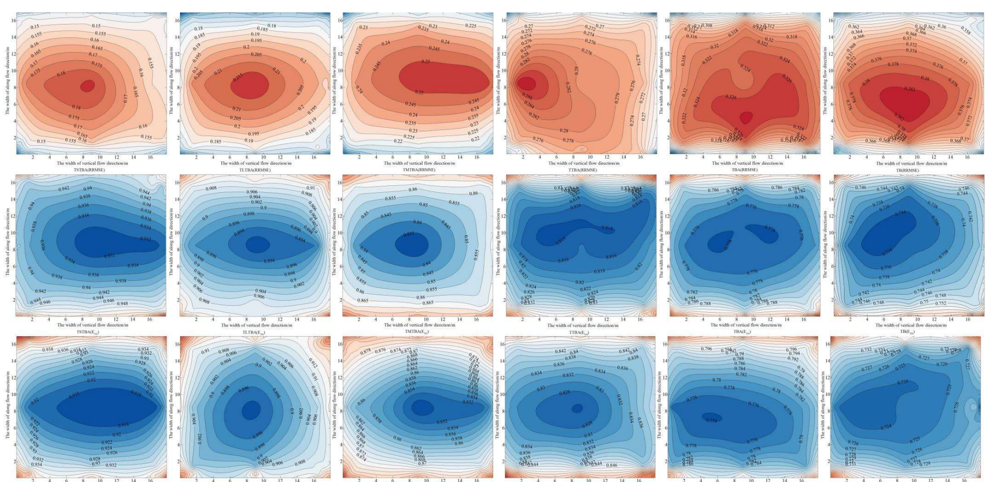

Figure 9: The accuracy space distribution of the simulated temperature of the lower layer of the concrete slab using different models

In summary, the TSTBA model exhibits the highest accuracy in simulating concrete temperatures across various slab regions.

III. B. Discussion

In the field of temperature estimation for concrete structures, the application of deep learning technology has brought new breakthroughs to address the limitations of traditional methods. As research into the temperature variation patterns of concrete structures in complex environments continues to deepen, deep learning models, with their powerful data processing and feature extraction capabilities, have gradually become a research hotspot.

Long Short-Term Memory (LSTM), as one of the key models in deep learning, boasts a unique structural design that gives it significant advantages in processing time series data. LSTM comprises input gates, forget gates, update gates, and output gates, which work together to effectively control the flow of information, its inflow, outflow, and memory, thereby accurately extracting and retaining useful information from input data over the long term. Numerous studies [26]-[28] have shown that LSTM performs excellently in various time series analysis tasks, ensuring the accuracy of feature extraction when handling concrete temperature data. It can capture complex patterns of temperature changes during the pouring and curing processes of concrete, providing reliable foundational data for subsequent temperature predictions.

However, the LSTM model still faces some challenges in practical applications, such as overfitting and gradient vanishing. To overcome these issues, the Bidirectional Long Short-Term Memory (BiLSTM) network was introduced. BiLSTM improved the traditional LSTM model by introducing a bidirectional hidden layer. This structure allows the model to capture information from both past and future directions in time series, further enhancing its ability to acquire contextual information. In the context of concrete temperature prediction, BiLSTM can more comprehensively analyze temperature trends, not only considering the impact of previous temperatures on the current moment but also integrating potential future changes for a comprehensive judgment, thereby improving the accuracy of model calculations [29], [30].

Temporal Convolutional Networks (TCNs) also demonstrate unique advantages when processing time series data. By employing techniques such as causal convolution, dilated convolution, and residual connections, TCNs can effectively capture long-range dependencies in time series. Among these, dilated convolution expands the receptive field without increasing the number of parameters, enhancing the model's ability to capture long-term time series features. In applications related to photovoltaic operation and maintenance (as verified by existing research), TCNs have proven their effectiveness in extracting local features. Combining TCNs with BiLSTM models can leverage the strengths of both. The TCN is responsible for extracting temporal features from concrete temperature data, particularly focusing on fine-grained local feature extraction; BiLSTM, on the other hand, uses its bidirectional structure to further process and integrate these features, thereby enhancing the model's ability to comprehensively extract global and local features, making the combined model outperform traditional BiLSTM models in terms of performance. Additionally, the pooling layer structure in the TCN model reduces the spatial dimensions of feature maps, effectively mitigating the risk of overfitting and improving the model's robustness, making it more stable and reliable when dealing with complex and variable concrete temperature data [31], [32].

In addition to optimizing the model structure, improvements in data processing and feature extraction are also crucial for enhancing the accuracy of concrete temperature estimation models. The TimeGAN model is based on the principle of Generative Adversarial Networks (GANs), learning and replicating data structures through training generative and discriminative components. At the same time, TimeGAN incorporates a supervised learning mechanism, which is an innovation that allows it to excel in capturing temporal sequence features of training data. This ensures the continuity of input data over time series, providing more realistic and relevant temporal feature information for concrete temperature prediction [33], [34].

The attention mechanism simulates the attention patterns of the human brain, capable of adaptively assigning weights to different parts of input data. In the concrete temperature estimation model, the attention mechanism can focus on key input data segments, automatically filtering out relatively unimportant information, thereby enhancing the model's ability to pay attention to and extract important features. This mechanism not only helps improve the estimation accuracy of the model but also prevents it from getting stuck in local optima, allowing the model to more flexibly adjust and optimize in complex concrete temperature data environments [35], [36].

In terms of model optimization algorithms, the Sparrow Search Algorithm (SSA), as an intelligent swarm optimization algorithm, simulates the foraging behavior and predator evasion actions of sparrows. This algorithm has been widely applied in multiple fields [37], [38] and has achieved excellent results. In the concrete temperature estimation model, the SSA algorithm significantly improves the accuracy of the model by optimizing the network weights and hyperparameters. This paper further improves the SSA algorithm by adopting a global optimization strategy, enhancing the algorithm's performance from multiple dimensions. Experimental results show that after improvement, the relative root mean square error (RRMSE) of the optimized SSA algorithm is reduced by at least

20.30%, while the efficiency coefficient (ENS) and coefficient of determination (NS) values are increased by at least 3.51%, greatly improving the overall performance of the model.

IV. Conclusions

Based on the measured temperature data of the concrete slabs of Yujin Weir in Jianzhong Irrigation District, this study constructed a hybrid deep learning model based on Bidirectional Long Short-Term Memory Network (BiLSTM) and Temporal Convolutional Network (TCN). It is optimized by using the globally improved Sparrow Search Algorithm (SSA), Ivy Optimization Algorithm (IvL), and Moss Growth Optimization Algorithm (MGO). Meanwhile, the TimeGAN model and attention mechanism are integrated, dedicated to improving the estimation accuracy of winter concrete temperature. From the perspective of in-depth analysis of model performance, the BiLSTM model, with its bidirectional structure, can simultaneously capture the forward and backward information of the time series, effectively overcoming the problem of incomplete information extraction of the traditional LSTM model when dealing with complex time series, and providing richer context information for the analysis of the temperature change trend of concrete. The TCN model performs well in extracting long-distance dependencies of time series through causal convolution, dilated convolution and residual connection. Moreover, the pooling layer structure effectively alleviates the risk of overfitting and enhances the robustness of the model. The combination of the two and their complementary advantages enable the basic model to have a strong feature extraction ability and better explore the potential patterns in the concrete temperature data.

The further introduced TimeGAN model, based on the architecture of Generative Adversarial Network (GAN), learns the data structure by training the generator and discriminator, and integrates the supervised learning mechanism at the same time. It can capture the time series characteristics of the training data more accurately and ensure the continuity of the input data in the time dimension. It provides more reliable time characteristic information for temperature prediction. The attention mechanism simulates the human attention pattern and can adaptively assign weights to different parts of the input data, focus on key information, automatically filter out irrelevant or secondary information, significantly enhance the model's attention to the characteristics of important data, avoid falling into local optimal solutions, thereby improving the prediction accuracy and generalization ability of the model.

In terms of model optimization, the improved SSA algorithm comprehensively enhances the global search ability and convergence speed of the algorithm through the initialization of chaotic sequence mapping, the butterfly optimization strategy to improve the explorer update, the sinusoidal and cosine search strategy to optimize the follower pose update, and the use of Gaussian distribution to improve the reconnaissance and early warning position update, making the model more efficient in the process of finding the optimal solution. It can better adjust the network weights and hyperparameters, thereby improving the model performance. The IvL algorithm simulates the growth, reproduction and diffusion mechanisms of ivy, while the MGO algorithm draws on the growth and reproduction processes of moss. These two algorithms, from different bio-inspired perspectives, provide diverse search strategies for model optimization, which helps the model break away from local optima and find a better solution space. Jointly promoted the adaptability and predictive ability of the model to complex concrete temperature data.

By comprehensively evaluating the performance of each model, the TSTBA model stands out in the estimation of concrete temperature. Its maximum deviation is only 0.648° C. This data indicates that when this model predicts the temperature of concrete, the deviation from the actual measured value is extremely small, and it can accurately reflect the real changes in the temperature of concrete. In terms of the relative root Mean square Error (RRMSE), its range is from 0.099 to 0.191, which means that the error fluctuation between the predicted value of the model and the actual value is small, and the prediction result is relatively stable and reliable. The coefficient of determination (R^2) reflects the goodness of fit of the model to the data. The R^2 range of the TSTBA model is from 0.930 to 0.979, indicating that this model can explain most of the reasons for the temperature changes of concrete and has a good fitting effect on the data. The efficiency coefficient (NS) is used to evaluate the simulation effect of the model. The NS range of the TSTBA model is from 0.916 to 0.970, indicating that the model can effectively capture the changing trend of the data during the simulation of concrete temperature, and the simulation results are highly consistent with the actual situation. In contrast, although the TLTBA and TMTBA models also have a certain degree of accuracy, they are inferior to the TSTBA model in terms of deviation control, error fluctuation, and the interpretation and simulation effect of data.

In conclusion, the TSTBA model demonstrates outstanding comprehensive performance, featuring high accuracy, stability and reliability. It can effectively capture the temperature variation patterns of concrete and serve as a reliable tool for estimating the temperature of concrete in winter. It provides strong technical support for the monitoring and control of concrete temperature in related fields such as water conservancy projects. It helps to ensure the safety and stability of concrete structures during winter construction and use.

Acknowledgments

This study was funded by Water Science and Technology Project of Hebei Province (2024-39) and Science Research Project of Hebei Education Department (BJ2021056).

References

[1] Svintsov, A. P., Shchesnyak, E. L., Galishnikova, V. V., Fediuk, R. S., Stashevskaya, N. A, 2020. Effect of nano-modified additives on properties of concrete mixtures during winter season. Construction and Building Materials, 237, 117527.

[2] Bai, X., Guan, J., Jiang, L., Fan, Z., Gao, Y., Qiao, T., 2024. Thermal performance study of straw concrete external walls for rural residences in hot-summer and cold-winter zone of China. Energy and Buildings, 311, 114140.

[3] Tan, Y., Tang, K., 2024a. Evaluate the effect of coarse aggregates on cement hydration heat and concrete temperature modelling using isothermal calorimetry. Heliyon, 10(19), e38322.

[4] Xu, W., Zhang, Y., Zhang, Y., Wang, Q., Li, Y., 2025. Prediction of temperature distribution in manufactured sand concrete based on hydration-temperature coupling model. Journal of Building Engineering, 101, 111961.

[5] Chen, H., Zhou, S., Deng, F., Zou, J., Wu, X., Fu, Z., 2017. Novel concrete-temperature monitoring method by using embedded passive wireless sensor. Magazine of Concrete Research, 70(9), 452-458.

[6] Adresi, M., Pakhirehzan, F., 2023. Evaluating the performance of Self-Sensing concrete sensors under temperature and moisture variations-a review. Construction and Building Materials, 404, 132923.

[7] Do, T. A., Nguyen, D. P., Hoang, V. H., Vu, B. T., Nguyen-Le, D. M., Nguyen, C. T., 2024. Effective applications of 1-D finite difference modeling for temperature prediction of concrete structures. Results in Engineering, 23, 102485.

[8] Zhang, Z., Tian, Z., Wu, Z., Xu, B., 2024. Development and analysis of a BP-LSTM-Kriging temperature field prediction model for the arch ring section of the reinforced concrete arch bridge. Structures, 64, 106564.

[9] Zhong, A., Sofi, M., Lumantarna, E., Zhou, Z., Mendis, P., 2023. A simplified numerical model for the temperature profile of early-age concrete. Magazine of Concrete Research, 1-13.

[10] Ge, P., Yang, O., Hua, X., Chen, Z., He, J., Liu, Z., Zhang, K., 2024. Predicting bond strength of corroded reinforced concrete after high-temperature exposure: A stacking model and feature selection. Construction and Building Materials, 456, 139290.

[11] Zhang,Y. P., Chu, Y. H., Zou, J. Y., Yu, C. Y., 2025. Machine learning prediction of steel–concrete composite beam temperatures during hot asphalt paving. Measurement, 242, 116257.

[12] Abid, S. R., Taysi, N., Özakca, M., 2016. Experimentalanalysis of temperature gradients in concrete box-girders. Construction and Building Materials, 106, 523-532.

[13] Sheng, X., Zhou, T., Huang, S., Cai, C., Shi, T., 2022. Prediction of vertical temperature gradient on concrete box-girder considering different locations in China. Case Studies in Construction Materials, 16, e01026.

[14] Tan, B., Wang, D., Shi, J., Zhang, L., 2024. Temperature field prediction of steel-concrete composite decks using TVFEMD-Stacking ensemble algorithm. Journal of Zhejiang University-SCIENCE A, 25(9), 732-748.

[15] Wang, X., Zhang, Y., Liu, Q., Wang, H., 2024. Prediction of the Pore-Pressure Built-Up and Temperature of Fire-Loaded Concrete with Pix2Pix. Computers, Materials and Continua, 79(2), 2907-2922.

[16] Bai, S., Kolter, J. Z., Koltun, V., 2018. An empirical evaluation of generic convolutional and recurrent networks for sequence modeling. arXiv preprint arXiv, 2018, 1803, 01271.

[17] Zhang, Y., M., Wang, H., 2023. Multi-head attention-based probabilistic CNN-BiLSTM for day-ahead wind speed forecasting. Energy, 2023, 278, 127865.

[18] Zhao, T., Jiang, B., Li, Y., Rezgui, Y., Zhang, C., Wang, P., 2025. Multi-point temperature or humidity prediction for office building indoor environment based on CGC-BiLSTM deep neural network. Building and Environment, 267, 112259.

[19] Xue, J. K., Shen, B., 2020. A novel swarm intelligence optimization approach: sparrow search algorithm[J]. Systems Science & Control Engineering, 8(1), 22-34.

[20] Ghasemi, M., Zare, M., Trojovský, P., Rao, R. V., Trojovská, E., Kandasamy, V., 2024. Optimization based on the smart behavior of plants with its engineering applications: Ivy algorithm. Knowledge-Based Systems, 295, 111850.

[21] Zheng, B., Chen, Y., Wang, C., Heidari, A. A., Liu, L., Chen, H., 2024. The moss growth optimization (MGO): concepts and performance. Journal of Computational Design and Engineering, 11(5), 184-221.

[22] Yin, L., Zhang, B., 2021. Time series generative adversarial network controller for long-term smart generation control of microgrids. Applied Energy, 281, 116069.

[23] Wang, Q., Chen, A., Cai, W., Cai, C., Fang, S., Li, L., Wang, Y. F., Zhou, G., 2023. Segmentation network of concrete cracks with multi-frequency OctaveRes dual encoder and cross-attention mechanism optimized by average weight. Automation in Construction, 155, 105050.

[24] Desideri, U., Zepparelli, F., Morettini, V., Garroni, E., 2013. Comparative analysis of concentrating solar power and photovoltaic technologies: technical and environmental evaluations. Appl Energy 102, 765–784.

[25] Feng, Y., Gong, D., Zhang, Q., Jiang, S., Zhao, L., Cui, N., 2019b. Evaluation of temperature-based machine learning and empirical models for predicting daily global solar radiation. Energy Conversion and Management, 198, 111780.

[26] Datta P, Faroughi S. A Multihead Lstm Technique for Prognostic Prediction of Soil Moisture. Geoderma, 2023, 433, 116452.

[27] Zhou, N., Shang, B., Xu, M., Peng, L., Feng, G., 2024. Enhancing photovoltaic power prediction using a CNN-LSTM-attention hybrid model with Bayesian hyperparameter optimization. Global Energy Interconnection, 7(5), 667-681.

[28] Tarafdar, A., Mahato, J., Upadhyay, R. K., Bhattacharya, P., 2025. Exploring the synergy of media awareness and quarantine classes in SiSAQEIHR model for pandemic control: A Deep LSTM-RNN predictions. Physica D: Nonlinear Phenomena, 134563.

[29] Dong, J., Zhu, Y., Cui, N., Jia, X., Guo, L., Qiu, R., Shao, M. A., 2024. Estimating crop evapotranspiration of wheat-maize rotation system using hybrid convolutional bidirectional Long Short-Term Memory network with grey wolf algorithm in Chinese Loess Plateau region. Agricultural Water Management, 301, 108924.

[30] Liu, X., Li, J., Liu, J., Huang, C., Liu, L., 2024. Prediction of permanent deformation of subgrade soils under ft cycles using sabo-optimized cnn-bilstm network. Case Studies in Construction Materials, 21, e03807.

[31] Pan, M., Fu, C., Cao, X., Guan, W., Liang, L., Li, D., Gu, J. K., Tan, D. L., Zhang, Z. Q., Man, X. J., Ye, N. Y., Qin, H., 2024. An energy management strategy for fuel cell hybrid electric vehicle based on HHO-BiLSTM-TCN-self attention speed prediction. Energy, 307, 132734.

[32] Pang, S., Zou, L., Zhang, L., Wang, H., Wang, Y., Liu, X., Jiang, J., 2025. A hybrid TCN-BiLSTM short-term load forecasting model for ship electric propulsion systems combined with multi-step feature processing. Ocean Engineering, 316, 119808.

[33] Li, Q., Zhang, X., Ma, T., Liu, D., Wang, H., Hu, W., 2022. A Multi-step ahead photovoltaic power forecasting model based on TimeGAN, Soft DTW-based K-medoids clustering, and a CNN-GRU hybrid neural network. Energy Reports, 8, 10346-10362.

[34] Sim, Y. S., Lee, C. K., Hwang, J. S., Kwon, G. Y., Chang, S. J., 2025. AI-based remaining useful life prediction for transmission systems: Integrating operating conditions with TimeGAN and CNN-LSTM networks. Electric Power Systems Research, 238, 111151.

[35] Lu, X. Q., Tian, J., Liao, Q., Xu, Z. W., Gan, L., 2024. CNN-LSTM based incremental attention mechanism enabled phase-space reconstruction for chaotic time series prediction. Journal of Electronic Science and Technology, 22(2), 100256.

[36] Yu, C., Li, Y., Zhai, G., 2025. Time-frequency attention mechanism-based model for enhancing wind speed prediction accuracy. Expert Systems with Applications, 265, 126038.

[37] Jia, Y., Su, Y. J., Zhang, R., Zhang, Z. N., Lu, Y. K., Shi, D. X., Xu, C. Q., Huang, D. F., 2022. Optimization of an extreme learning machine model with the sparrow search algorithm to estimate spring maize evapotranspiration with film mulching in the semiarid regions of China. Computers and Electronics in Agriculture, 201, 107298.

[38] Lei, L., Shao, S. L., Liang, L. X., 2024. An evolutionary deep learning model based on EWKM, random forest algorithm, SSA and BiLSTM for building energy consumption prediction. Energy, 288, 129795.